the polarization controllers on both arms. The beat signal is then amplified by an erbium-doped fiber amplifier (EDFA) with 33-dBm maximum output power to generate sufficient optical intensity for observing the nonlinear effect. The power is coupled into and out of the waveguide through lensed fibers. The optical spectrum due to SPM is analyzed by an optical spectrum analyzer while the power is measured by a power meter.

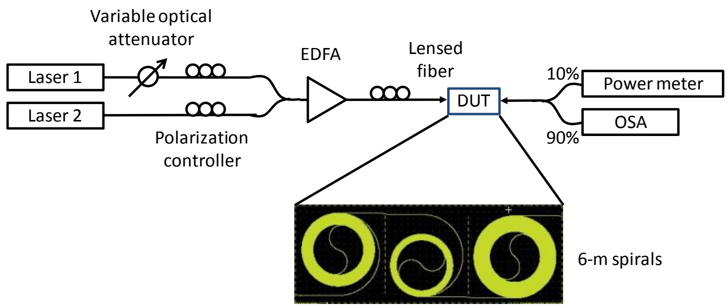

Fig. 3. Nonlinearity measurement setup using CW SPM method.

A measured SPM spectrum for TE-polarized light through a 6-m long spiral waveguide is shown in Fig. 4. With 29-dBm beat signals launched into the waveguide, the nonlinear effect is observed through the spectrum. The nonlinear phase shift is extracted from the relative intensity of the fundamental wavelength and the first-order sideband. The relation between the nonlinear phase shift and the intensity is given as [1]

$$\frac{I_0}{I_1} = \frac{J_0^2(\varphi_{SPM}/2) + J_1^2(\varphi_{SPM}/2)}{J_1^2(\varphi_{SPM}/2) + J_2^2(\varphi_{SPM}/2)}, \tag{13}$$

where I_0 and I_1 are the intensities of the fundamental wavelength and the first-order sideband, J_n is the Bessel function of the *nth* order, and φ_{SPM} is the nonlinear phase shift due to SPM. The phase shift only depends on the intensity ratio between the fundamental wavelength and the first-order sideband. It is independent of the laser linewidth and the wavelength separation of the two lasers if the chromatic dispersion is negligible. To neglect the chromatic dispersion, the wavelength separation and the waveguide length must be small enough [1,9]. We also experimentally confirmed the influence of dispersion is negligible by tuning the wavelength separation of the lasers.

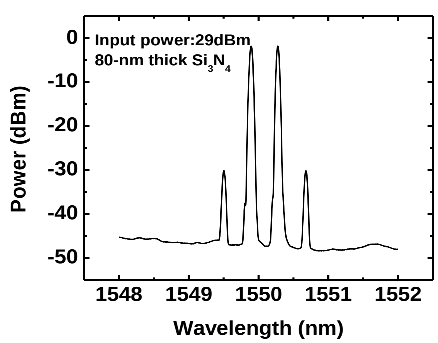

Fig. 4. SPM spectrum through a 6-m long spiral waveguide with 2.8 µm of core width and 80 nm of core thickness. The input light is TE-polarized with optical power of 29 dBm.

The relation between the nonlinear phase shift and input optical power for three test chips with different waveguide core thicknesses (80 nm, 90 nm, and 100 nm) is shown in Fig. 5. It should be mentioned that the nonlinearity from the EDFA was measured and subtracted when characterizing the waveguide nonlinearity. The waveguide with thicker core exhibits larger nonlinear phase shift because of its smaller effective core area and thus stronger intensity.

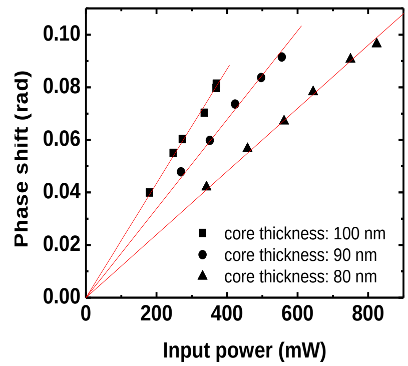

Fig. 5. Measured nonlinear phase shifts at various input powers for different Si_3N_4 core thicknesses. The solid lines are linear fitting of the measurements.

Once the nonlinear phase shift is known, the nonlinear coefficient γ and effective n_2 are derived from the slope of the fitted straight lines in Fig. 5, and plotted in Fig. 2 and Fig. 6 using the following formula [8].

$$\varphi_{SPM} = \frac{2\pi}{\lambda} \frac{n_{2,eff}}{A_{eff}} L_{eff} P_{in} = \gamma L_{eff} P_{in}, \tag{14}$$

where P_{in} is the waveguide input power and L_{eff} is the effective length defined as

$$L_{eff} = \frac{\left(1 - e^{-\alpha L}\right)}{\alpha}, \tag{15}$$

where L is the actual length of the waveguide and α is the waveguide loss. The squares in Fig. 2 and Fig. 6 are measurement data points from six test chips with three different Si_3N_4 core thicknesses while the solid lines represent the calculated nonlinearity as described in Section 2. The nonlinear refractive index coefficients n_2 for Si_3N_4 and SiO_2 are 3.5×10^{-15} cm^2/W and 2×10^{-16} cm^2/W, respectively, for calculation [1,10]. When the core thickness is reduced, the optical mode of the waveguide is squeezed out and more optical power overlaps with the SiO_2 cladding. Therefore, the effective n_2 is closer to n_2 of SiO_2 with reduced core thickness. The measured γ and effective n_2 are a little less than the theoretical prediction because a thin silicon oxynitride layer may occur at the interface of Si_3N_4 and SiO_2 because of nitrogen diffusion during the thermal annealing step of waveguide fabrication [11]. This influence is more obvious especially for a very thin Si_3N_4 layer. It should also be mentioned that all the waveguide nonlinearity is measured with TE-polarized optical input because the waveguide is designed to support fundamental TE mode only. The loss of TM mode is much larger than that of TE mode; therefore, it is not possible to characterize the waveguide nonlinearity with TM-polarized optical input.

#133525 - $15.00 USD   Received 17 Aug 2010; revised 22 Oct 2010; accepted 22 Oct 2010; published 26 Oct 2010

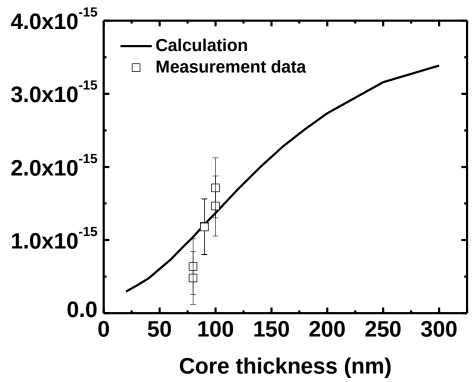

Fig. 6. Effective n_2 for different core thicknesses. The solid lines represent the theoretical calculation using the perturbation theory while the squares represent the measured data points.

For the application of optical delay lines, low nonlinearity is required to have small power-dependent optical phase variation over a length of waveguide. Given a specific phase variation tolerance, we can estimate the maximum handling power for a waveguide. For our 80-nm-thick Si_3N_4 waveguides, the maximum affordable propagation power over 20-m long waveguides (100-ns delay) can be as large as 120 mW with phase variation less than π/20. It is feasible to propagate even higher power by reducing Si_3N_4-core thickness in order to lower the nonlinearity of waveguides, as indicated in Fig. 6.

4. Conclusions

We have demonstrated ultra-low loss Si_3N_4-core and SiO_2-cladding rectangular waveguides that are capable of handling high propagating power because of their low nonlinearity. The nonlinearity of the waveguide is described using effective n_2, which is derived by solving Maxwell's wave equation with introduced power-dependent refractive index perturbation. The effective n_2 of the waveguides with different core thicknesses is measured using CW SPM and shows agreement with the theoretical calculation of waveguide nonlinearity. The waveguide with 80-nm-thick core is characterized, and has effective n_2 of about 9×10^{-16} cm^2/W, which can handle 120-mW optical power over a length of 20 meters with negligible power-dependent phase variation.

Acknowledgements

The authors thank Scott Rodgers, Daoxin Dai, Zhi Wang, and Paolo Pintus for helpful discussions. This work is supported by DARPA MTO under iPhoD contract No: HR0011-09-C-0123.

#133525 - $15.00 USD Received 17 Aug 2010; revised 22 Oct 2010; accepted 22 Oct 2010; published 26 Oct 2010